LIMNOLOGY
and
OCEANOGRAPHY

ASLO

Limnol. Oceanogr. 65, 2020, 413–425

doi: 10.1002/lno.11311

Successional blooms of alkenone-producing haptophytes in Lake George, North Dakota: Implications for continental paleoclimate reconstructions

Susanna Theroux,[1,2,a] Yongsong Huang,[1] Jaime L. Toney,[3] Robert Andersen,[4] Paul Nyren,[5] Rick Bohn,[5] Jeffrey Salacup,[1,6] Leslie Murphy,[2] Linda Amaral-Zettler [1,2,7,8*]

[1]Department of Earth, Environmental and Planetary Sciences, Brown University, Providence, Rhode Island
[2]The Josephine Bay Paul Center for Comparative Molecular Biology and Evolution, Marine Biological Laboratory, Woods Hole, Massachusetts
[3]School of Geographical and Earth Sciences, University of Glasgow, Glasgow, UK
[4]Friday Harbor Laboratories, University of Washington, Friday Harbor, Washington
[5]Central Grasslands Research Extension Center, North Dakota State University, Streeter, North Dakota
[6]Department of Geosciences, University of Massachusetts, Amherst, Massachusetts
[7]Department of Freshwater and Marine Ecology, Institute for Biodiversity and Ecosystem Dynamics, University of Amsterdam, Amsterdam, The Netherlands
[8]Department of Marine Microbiology and Biogeochemistry, NIOZ Royal Netherlands Institute for Sea Research & Utrecht University, Den Burg, The Netherlands

Abstract

Alkenone-derived paleotemperature reconstruction holds great promise in lake environments. However, the occurrence of multiple species of alkenone-producing haptophyte algae in a single lake can complicate the translation of alkenone unsaturation to temperature if each species requires an individual temperature calibration. Here, we present the first systematic monitoring of two alkenone-producing haptophytes throughout the course of a seasonal cycle in Lake George, North Dakota, using a combined approach of DNA sequencing and alkenone lipid characterization. Field sampling revealed a nonoverlapping haptophyte succession, with both an early and late season haptophyte bloom event. Culturing experiments demonstrated that the two haptophyte species responsible for these blooms had statistically similar alkenone-temperature responses, although the culture-based calibrations were distinct from the in situ calibration. Bloom timing of each haptophyte species corresponded to surface-water temperatures that differed by more than 10°C, revealing that changes in bloom intensities for each species will skew the sediment-inferred temperatures to a different stage of the growth season. These results highlight the importance of accounting for bloom timing when interpreting alkenone-derived temperatures in sediment cores, especially in lakes that experience large seasonal fluctuations in water column temperature and salinity.

For more than three decades, long-chain alkenones produced by haptophyte algae have provided climate scientists with a glimpse into ancient aquatic environments (Brassell et al. 1986; Prahl and Wakeham 1987). The relative proportions of di-($C_{37:2}$), tri-($C_{37:3}$), and tetra-($C_{37:4}$) unsaturated alkenones are known to reflect algal growth temperatures and form the basis of the U^K_{37} paleotemperature proxy (Marlowe et al. 1984; Brassell et al. 1986). The modified $U^{K'}_{37}$ proxy (Prahl et al. 1988) omits the tetra-unsaturated alkenones and is widely used for interpreting marine paleoclimate records, and the recently defined $U^{K''}_{37}$ (Zheng et al. 2016) omits the di-unsaturated alkenones and was developed for use in freshwater and brackish water.

Alkenone production is restricted to haptophyte algae in the order Isochrysidales and alkenone-producing species have been categorized into three main groups based on phylogenetic relationships and commonly associated habitats (Theroux et al. 2010; Longo et al. 2016). Group I alkenone-producing haptophytes

*Correspondence: linda.amaral-zettler@nioz.nl

Additional Supporting Information may be found in the online version of this article.

[a]Present address: Southern California Coastal Water Research Project, Costa Mesa, California

(hereafter, Group I) have been found in fresh and oligohaline lakes (Theroux et al. 2010; Simon et al. 2013; Longo et al. 2016), and are believed to only occupy environments with salinities lower than ~ 5 psu (Longo et al. 2016). Group II alkenone-producing haptophytes (Group II) are common in brackish and saline lakes and coastal environments, and Group III alkenone-producing haptophytes (Group III) are common in open ocean marine environments (Theroux et al. 2010; Longo et al. 2016). Group III haptophytes include the cosmopolitan species *Emiliania huxleyi* and its close relative *Gephyrocapsa oceanica*, both responsible for producing the majority of marine alkenones (Volkman et al. 1980; Marlowe et al., 1984; Volkman et al. 1995). Alkenones produced by Group I haptophytes differ structurally from those produced by Group II and III and are characterized by the unusual alkenone double bond positional isomers (Longo et al. 2013; Dillon et al. 2016), allowing for rapid identification of Group I haptophytes by alkenone profile.

A narrow phylogenetic range in marine alkenone-producers allows for the application of a universal $U^{K'}_{37}$ calibration for sea surface temperature reconstructions, a calibration that was first developed empirically through culture work (Brassell et al. 1986; Prahl and Wakeham 1987) and later validated with a global core-top survey (Müller et al. 1998; Conte et al. 2006). For freshwater environments where Group I haptophytes have been identified, namely a series of arctic lakes in Greenland (D'Andrea et al. 2011) and Alaska (Longo et al. 2016), studies have found a uniform species occurrence that allows for a consistent temperature calibration to be applied in individual lakes. In Lake BrayaSø, Greenland, for example, an in situ U^{K}_{37} calibration derived from a single haptophyte species matched a downcore alkenone profile spanning 6000 yr (Theroux et al. 2010, 2012; D'Andrea et al. 2011). The BrayaSø sediment record presents an ideal environment for an alkenone-based paleotemperature reconstruction wherein a single in situ-derived index calibration can be applied back through time (D'Andrea et al. 2006, 2011; Theroux et al. 2010, 2012).

In contrast, brackish and saline lake environments have been shown to harbor multiple Group II haptophyte lineages, complicating the applicability of a universal calibration. Like their marine and freshwater counterparts, alkenone unsaturation ratios in Group II haptophytes display excellent linear relationships to growth temperatures when cultured individually (Versteegh et al. 2001; Sun et al. 2007; Toney et al. 2010; Theroux et al. 2013; Nakamura et al. 2016; Zheng et al. 2016; Araie et al. 2018). However, when multiple species co-occur in an environment, each species may require a separate U^{K}_{37} calibration, as well as a measure of relative abundance or productivity to detangle mixed alkenone signatures. For example, surface sediment DNA sequencing in Ace Lake, Antarctica (Coolen et al. 2004) and lakes on the Tibetan plateau and Great Plains of the United States (Theroux et al. 2010; Toney et al. 2012) revealed multiple, co-occurring haptophyte populations. In the Black Sea (Coolen et al. 2009), alternating alkenone profiles in downcore sediment horizons suggested fluctuations in dominant haptophyte populations, likely responding to variations in sea surface salinity.

The central rationale for the current study stems from our previous investigations of alkenones and haptophyte species in brackish Lake George, North Dakota. DNA sequencing efforts in Lake George revealed the presence of two distinct alkenone-producing haptophyte species, designated Hap-A and Hap-B (Theroux et al. 2010; Toney et al. 2012). Hap-A is a close relative of haptophytes from Ace Lake, Antarctica and the cultured species *Isochrysis galbana* 8701 and newly resolved *Tisochrysis lutea* CCAP927/14 (Theroux et al. 2010; Bendif et al. 2013). Hap-B is a close relative of cultured haptophyte *Ruttnera* (*Chrysotila*) *lamellosa* (Theroux et al. 2010). The Lake George in situ water column alkenone calibration revealed a strong linear relationship to temperature (Toney et al. 2012; Zheng et al. 2016), although the contribution of alkenones from each of the two haptophyte species remains unknown. To this end, we developed this study to better understand the influence of multiple alkenone-producing haptophyte species on a single alkenone sediment record.

We hypothesized that the seasonal timing of haptophyte species blooms can strongly impact the interpretation of the resulting lake sediment record. To gain an improved understanding of the timing and provenance of haptophyte-derived alkenones, our study aims to: (1) determine the timing of blooms for the two different haptophyte species in Lake George over a seasonal cycle, (2) identify co-occurring eukaryote populations to better understand bloom triggers, and (3) compare the temperature sensitivities of the two haptophyte species using in situ water column samples and laboratory cultures. To achieve these goals, we sampled the 2011 Lake George water column during the haptophyte spring/summer bloom and analyzed the geochemical and biological signatures of the bloom. We used high-throughput DNA sequencing and culture manipulations to gauge haptophyte succession and alkenone production. Our study provides the first comprehensive in situ analysis of haptophyte species succession during a lacustrine bloom event and uncovers how seasonal amplitude is imprinted in the lake sedimentary record.

Methods

Site description

Lake George (46.74°N, 99.49°W) is situated in the Northern Great Plains in ND, U.S.A. (Fig. 1). Lake George has a maximum depth of 60 m and an average salinity of 9.72 ppt, both of which contribute to its well-preserved lake sediment records (Eisenlohr and Sloan 1968; Fritz 2011), in addition to an average pH of 8.98 (Toney et al. 2010). Glacial retreat formed the lake over 12,000 yr ago, and the lake's salinity is likely maintained by input from deep sources of saline groundwater (Fritz 2011). Lake George sits atop the Hell Creek, Fox Hills and Pierre formations of the Upper Cretaceous (Whitehead 1996), and sources its high sulfate concentrations (7370 mg L^{-1}) from the oxidation of pyrite in the Pierre shale.

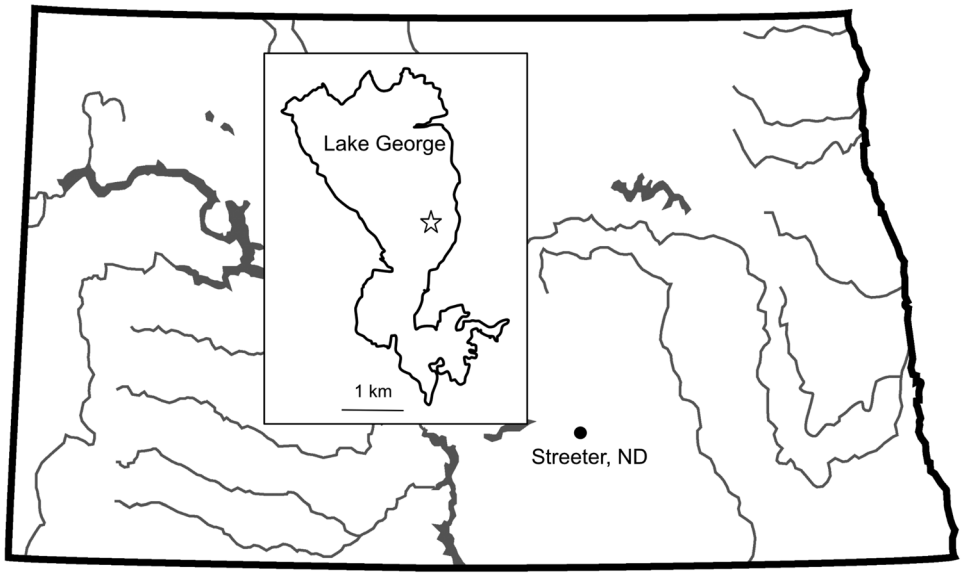

Fig. 1. Map of North Dakota and Lake George (inset) with sampling location indicated by a star.

Bloom sampling

From April through July 2011, we sampled the waters of Lake George bimonthly to gauge haptophyte populations and alkenone abundance throughout the course of the spring and summer seasons. We collected water using a Van Dorn water sampler at 0, 5, and 10 m depths. From each depth, we collected 1 L each for DNA analysis, alkenone analysis, and geochemical analyses. For alkenone analysis, we filtered 1 L of water onto a precombusted (550°C) Whatman GF/F 0.7-μm, 47-mm glass fiber filter (GE, Marlborough, MA) and kept it frozen at −20°C until analysis. For DNA analysis, we filtered a liter of lake water onto a 0.2-μm Sterivex™ filter (Millipore, Billerica, MA, U.S.A.), flooded the filter with Puregene lysis buffer (Qiagen, Valencia, CA, U.S.A.), and froze it at −20°C until processing. For geochemical analyses, we filtered water through a 0.2-μm Whatman Nucleopore polycarbonate filter (GE, Marlborough, MA) to remove microbes and particulate matter and stored samples at −20°C until processing.

Geochemical analysis

We used a YSI 85 sonde (YSI Life Sciences, Yellow Springs, OH) to measure lake water temperature, pH, dissolved oxygen (DO), and conductivity in situ. We measured nitrate, nitrite, and phosphate from 0.2 μm-filtered water using a Westco Smartchem 200 Discrete Analyzer (Brookfield, CT) at Brown University, RI. Cation and anions were analyzed at the Barnstable County Department of Health and Environment Laboratory (Barnstable, MA) using an Agilent ICP-MS EPA (Method 200.8) and a Perkin Elmer Flame Atomic Absorption Spectrometer (Waltham, MA).

Hap-A enrichment culture U^K_{37} calibration

We initiated a sediment enrichment culture after Toney et al. (2012) by overlaying 50 g Lake George surface sediment in a sterile glass beaker with 2 L of 0.2-μm filtered Lake George water amended with f/2-Si nutrients (Guillard 1975). We grew the sediment enrichment culture in a 4°C incubator with a 24:0 light:dark light regime using full-spectrum lighting (Full Spectrum Solutions, Jackson, MI). Haptophytes preferentially metabolize more unsaturated alkenones when in the dark and the constant illumination was used to avoid a degradation bias. After 4 weeks, we subsampled the enrichment culture supernatant and separated this subculture into < 3, 3–5, and 5–10 μm size fractions using Millipore Isopore cellulose nitrate filters (Billerica, MA). We filtered each size fraction onto a 44-mm GFF Whatman filter for alkenone analysis and kept the filter at −20°C until extraction. We detected alkenones in only the < 3 μm fraction and used this fraction for a temperature manipulation experiment.

We grew the < 3 μm subcultures in sterile glass culture tubes in 0.2 μm-filtered Lake George water amended with f/2-Si nutrients (Guillard 1975). We grew the cultures in volumes of 50 mL at 5°C, 10°C, 15°C, 21°C, and 24°C under 24:0 light:dark regime using a full-spectrum light. All cultures were inoculated with approximately 8000 cells mL^{-1} after a 2-week acclimation to growth temperature. The cultures were sampled biweekly for cell counts and cell concentrations were determined using a hemocytometer to ensure the cultures were maintained in the logarithmic growth phase. At the end of 3 weeks, we harvested 50 mL of culture for alkenone analysis by filtering onto a 44-mm GFF Whatman filter and freezing the filter at −20°C until extraction.

Culture studies to determine Hap-B U^K_{37} calibration

We achieved a clonal culture of haptophyte Hap-B (#A12,903, Roscoff Culture Collection RCC4060, *Ruttnera* cf. *lamellosa*) through cell isolation with sterilized glass pipettes. We grew this

clonal culture in glass vials in 0.2-μm filtered Lake George water amended with f/2-Si nutrients (Guillard 1975) at 5°C, 10°C, 15°C, 21°C, and 24°C under 24:0 light:dark regime using a full-spectrum light (Maxum™ 5000 bulb, BlueMax, Jackson, MI). The cultures were sampled biweekly for cell counts and cell concentrations were determined using a hemocytometer to ensure the cultures were maintained in the logarithmic growth phase. At the end of 3 weeks, we harvested the cultures for alkenone analysis.

Alkenone extraction and analysis

Alkenone filters were freeze-dried before analysis and extracted using three 20-min bursts of sonication in dichloromethane. We ran the total lipid extracts on an Agilent 6890 plus Gas Chromatograph Flame Ionization Detector (Santa Clara, CA) for detection and quantification of alkenones. Two quantification standards (n-C_{36} and n-C_{37} alkanes) were added to all samples before being injected from an autosampler into a 112°C cooled injection system-programmed temperature vaporizer inlet operated in solvent vent mode. After the initial vent, the inlet was ramped at 12°C min^{-1} to 240°C, held isothermally for 5 min, ramped again at 12–320°C, and held isothermally for 2 min before cryogenic cooling. The oven began at 90°C for 2 min, was ramped at 40°C min^{-1} to 255°C, at 1–302°C, and at 10–325°C where it was held isothermally for 20 min. Hydrogen was used as a carrier gas, and the column was a 60 m, 0.32 mm internal diameter, 0.10-μm film DB-1 with a 5 m fused guard column (DB-1 Agilent Duraguard). Analytical accuracy was tracked via the injection of laboratory $U^{K'}_{37}$ standard of known temperature and equaled ± 0.042 $U^{K'}_{37}$ units (± 0.1°C). Outlier data points were identified using Cook's distance as implemented in the stats packages in the R program (R Core Team 2013).

DNA extraction and sequencing

We extracted the Sterivex DNA filters using a Gentra Puregene Cell Kit (Qiagen, Hilden, Germany) according to the manufacturer's instructions. Genomic DNA was further purified using the MoBio PowerClean Kit (MoBio, Carlsbad, CA) to remove polymerase chain reaction inhibitors. We quantified total extracted genomic DNA yields using a NanoDrop nucleic acid spectrophotometer (Thermo Scientific, Wilmington, DE).

For ion torrent (IT) sequencing of Lake George water samples, we performed genomic DNA amplifications using eukaryotic-specific primers 1380F/1389F and 1510R that target the 18S rRNA gene variable V9 region (Amaral-Zettler et al. 2009). We then ligated both barcodes and adapters to these V9 amplicons. We sequenced the amplicons using an Ion Torrent Personal Genome Machine with bidirectional sequencing at the Life Technologies facility. Minimum information about a marker gene sequence (MIMARKS) compliant data (Yilmaz et al. 2011) are deposited in NCBI's Sequence Read Archive (SRA: SRP144759), and sample metadata are included in Supporting Information Table S3. Operational taxonomic units (OTUs) for Hap-A and Hap-B can be found under GenBank accession numbers MN176134 and MN176135, respectively. We additionally sequenced the Hap-B culture isolate (#A12,903) to link both the field and culture Hap-B sequences (Supporting Information Methods). This additional Hap-B OTU can be found under accession number MN176143.

Sequence bioinformatics

Ion torrent DNA sequence reads were trimmed and screened for quality after Huse et al. (2007), including the paired end information as a measure of accuracy. Sequences were eliminated if they did not contain full forward and reverse primer sequences, or if they contained greater than one ambiguous base pair (N). We clustered the sequences at 97% similarity using SLP-PWAN (Huse et al. 2010) into OTUs. For each OTU, we selected a representative sequence to assign taxonomy. To assign taxonomy, we used the Global Alignment for Sequence Taxonomy (GAST) algorithm (Huse et al. 2008) and an in-house reference sequence database. We eliminated singleton OTUs with only one sequence representative. Our finished data set consisted of 1,018,154 sequence reads distributed across 3750 OTUs.

Results

Eukaryotic community during the bloom events

We identified 220 unique eukaryotic OTUs in the Lake George water column. Of these, copepod, ciliate, cercozoan, and chlamydomonad-related OTUs were the most abundant amplicon sequences recovered from all depths (Supporting Information Table S2). In both the surface waters and at 5 m depth, copepod, as well as *Chlamydomonas*, Fragilariaceae, and *Uroglena* OTUs were the numerically most abundant. A copepod was the most abundant OTU at 10 m depth, as well as an apicomplexan and the haptophyte *Pavlova*, a member of the Haptophyta that does not produce alkenones.

Seven haptophyte OTUs were recovered from all samples, four from the Pavlovales, two from Isochrysidales, and one from the Prymnesiales (Supporting Information Fig. S2). Across all samples, Pavlovales were numerically the most abundant haptophyte reads, with Isochrysidales abundant primarily in the surface waters. The two putative alkenone-producing haptophyte OTUs (Euk_03_47 and Euk_03_52) were designated Hap-A and Hap-B after previous sequencing work from Lake George cultures (Toney et al. 2012). Hap-A reads were most abundant in the surface waters on Day 10, although they exhibited greater abundance earlier in the season at 5 m and 10 m depths, suggesting a transit from surface sediments to the surface waters (Fig. 2). Hap-B reads increased at 0 m through the latter half of the sampling period (Fig. 2), with an apex at Day 42, and few numbers at either 5 or 10 m depth. No other haptophyte species exhibited a similar bimodal distribution in the water column throughout the season (Supporting Information Fig. S2). Given the concentrations of Hap-A and Hap-B in the water column, we defined

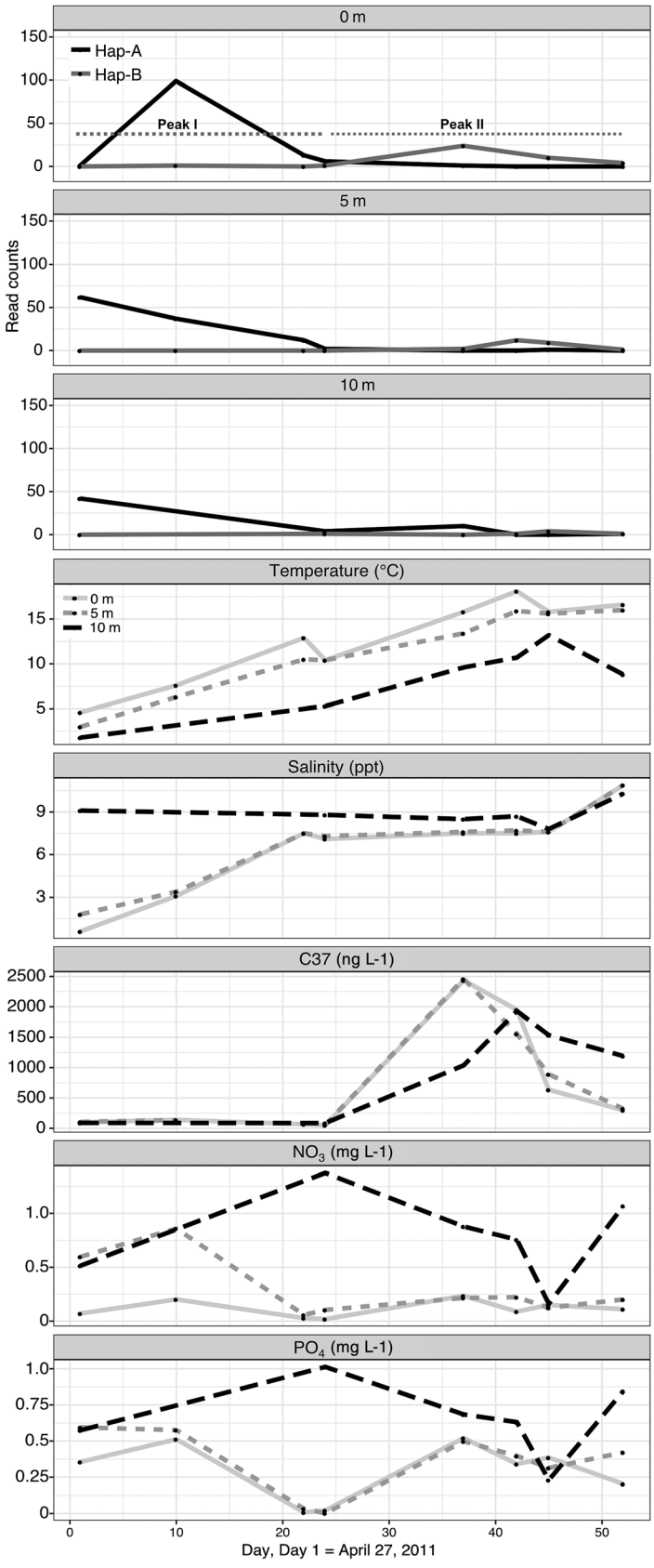

Peak I as spanning days 1–24 when Hap-A is dominant, and Peak II as spanning days 25–52 when Hap-B was dominant (Fig. 2).

Peak I and Peak II eukaryotic communities showed a clear separation in species membership (Fig. 3a). An indicator species analysis (Supporting Information Methods) revealed an enrichment in Hap-A and alveolates during Peak I (Supporting Information Table S2). Hap-B was an indicator species for Peak II, along with a *Pavlova* OTU and a few uncultured eukaryotes (Supporting Information Table S2). This analysis also revealed that there were almost no indicator species for depth, whereas salinity and temperature yielded multiple indicator species (Supporting Information Table S2). Multiple chlamydomonad OTUs were associated with low salinities (0–4 ppt). Low temperatures (1–6°C) saw an enrichment in alveolates and a Prymnesiales haptophyte, while Hap-B was an indicator species for the upper temperature range (13–19°C). At the upper temperatures, there was also an enrichment in a *Pavlova* OTU and a few stramenopile OTUs. The mid-temperature range (6–13°C) saw only a few indicator species, namely a diatom OTU and ciliate OTUs. Of the most abundant protistan species, Cryomonadida, Chlorophyta, and Hap-A species peaked during the late spring, whereas Bacillariophyta and Chrysophyceae OTU peaks preceded the Hap-B Peak II. Ciliate OTUs were the only other dominant group to peak synchronously with Hap-B sequences (Supporting Information Fig. S1).

Early blooming Hap-A was positively associated with Chlorophyta, Cercozoa, Chytridiomycota, Bacillariophyta OTUs and a few ciliate species, and weakly correlated to Dinophyta OTU abundances. Hap-A was strongly negatively associated with Hap-B, a *Planomonas micra* OTU (Euk_03_70), multiple Heterokontophyta and Cryptophyte OTUs, and a ciliate and Ochrophyta OTU (Supporting Information Fig. S6). In contrast, Hap-B was positively associated with the *P. micra* OTU, as well as Heterokontophyta OTUs that were negatively associated with Hap-A, in addition to several Ochrophyta and Opisthokonta OTUs. Hap-B was strongly positively associated with an unknown Cryptophyte OTU (Euk_03_20). Hap-B was negatively associated with numerous Chlorophyta OTUs, Cercozoan OTUs, and Eustigmatophyta and Bacillariophyta OTUs. Temperature, DO, calcium, and magnesium concentrations were responsible for shaping the Hap-A and Hap-B abundances, while temperature, salinity, and pH played a role in shaping the entire eukaryote community (Supporting Information Table S4).

Fig. 2. Lake George haptophyte and water chemistry conditions during sampling period, including rarefied IT sequence read counts of Hap-A and Hap-B throughout the seasonal cycle at 0, 5, and 10 m depths and Lake George water column temperature, salinity, C_{37}-alkenones, nitrate, and phosphate water column concentrations throughout the sampling period at 0, 5, and 10 m depths. Peak I and Peak II as indicated.

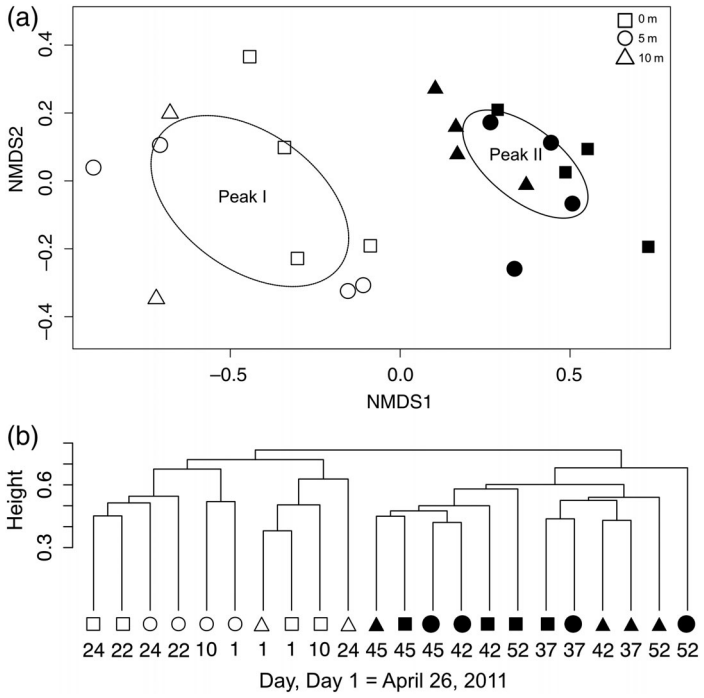

Fig. 3. (**a**) Nonmetric multidimensional scaling analysis and (**b**) average linkage clustering of all OTUs.

Water chemistry during bloom

Throughout the 2011 sampling period, C_{37} alkenones reached concentrations of over 2400 ng L^{-1} (Fig. 2), on par with concentrations observed during an Arctic lake haptophyte bloom (Theroux et al. 2012), but almost an order of magnitude lower than previously reported concentrations in Lake George (Toney et al. 2010). The C_{37} alkenone concentrations peaked at Day 10 (Peak I) and Day 37 (Peak II) in the surface waters, although the Peak II concentrations were an order of magnitude higher than the Peak I concentrations (Fig. 2). Tetra-unsaturated alkenones dominated the water column alkenone signature at almost all time points and all depths, except for Peak II surface waters that were dominated by tri-unsaturated alkenones (Supporting Information Table S1).

The water column experienced a gradual warming over the course of the sampling period, ranging from 5°C after ice-melt to 25°C in late July. Salinity plateaued in the first half of the summer and exhibited a second peak in the latter half of the seasonal cycle at all depths (Fig. 2). The lowest concentrations of nitrate and phosphate on Day 24 corresponded to the lowest alkenone concentrations in the water column and the break period between the two alkenone concentration peaks. Nitrate and phosphate concentrations were positively correlated with each other, and nutrient concentrations at 0 and 5 m depth also mirrored alkenone concentrations in Peak II (Supporting Information Table S3). Nitrate, phosphate, and DO were the only environmental variables that segregated by depth, while multiple variables, including pH, DO, salinity, and temperature, were significantly different between Peak I and Peak II (ANOVA, $p < 0.05$) (Supporting Information Table S6).

In situ alkenone distributions and U^K_{37} calibration

Combining the Lake George 2011 water temperatures and alkenone concentrations yielded an in situ Lake George U^K_{37} calibration defined by the equation:

$$U^K_{37} = \mathbf{0.0271\,T - 0.74} \quad (1)$$

where U^K_{37} is the concentration of $(C_{37:2}\text{-}C_{37:4})/(C_{37:2} + C_{37:3} + C_{37:4})$ and T is temperature in °C. This calibration had an R^2 value of 0.68 and a root mean squared error (RMSE) of 3.7°C (Fig. 4a) and had both a slope and y-intercept within one-hundredth of the Lake BrayaSø in situ calibration (0.025 and −0.779 respectively; D'Andrea et al. 2011). The largest scatter in the U^K_{37} calibration occurred around 10°C, with contributing alkenones at this temperature sourced from both Peak I and Peak II periods (Fig. 4a). Separating the Peak I and Peak II calibration data points did not improve the calibration, and Peak I data points alone did not yield a positive, linear U^K_{37} calibration (Fig. 4a). The recently reported $U^{K\prime\prime}_{37}$ index resulted in a slightly improved calibration, reaffirming the minimal influence of the $C_{37:2}$ alkenone (Fig. 4b). Separating the U^K_{37} calibrations by depth revealed the strongest calibrations at 0 and 5 m (Supporting Information Fig. S4). As expected, the percentage of $C_{37:4}$ alkenones decreases as temperature increases, and likewise showed a weak negative relationship with salinity (Supporting Information Fig. S5).

Culture studies and U^K_{37} calibrations

We attempted various isolation techniques to culture the two putative alkenone-producing haptophytes from Lake George (Theroux et al. 2010; Toney et al. 2012). We cultured Hap-A in an enrichment culture with other microbial consortia present, but we were unable to grow it as a pure, axenic culture. The size fractionation experiment determined that Hap-A cells were < 3 μm in size, qualifying it as a picoplankter for at least a portion of its growth cycle (Fig. 5). The Hap-A enrichment culture alkenones had a dominant $C_{37:4}$ signature at low temperatures (Table 1) and yielded a U^K_{37} calibration defined as:

$$U^K_{37} = \mathbf{0.037\,T - 0.76} \quad (2)$$

with an R^2 value of 0.95 and a RMSE value of 1.6°C. Cultures of Hap-B (#A12,903) grew successfully at all temperatures and demonstrated a characteristic increase in saturated alkenones with increasing temperatures (Table 1). Additional sequence data from the Hap-B culture covering a great portion of the 18S gene (GenBank #MN176143) allowed us to confirm the identity of the Hap-B environmental sequence (GenBank #MN176135),

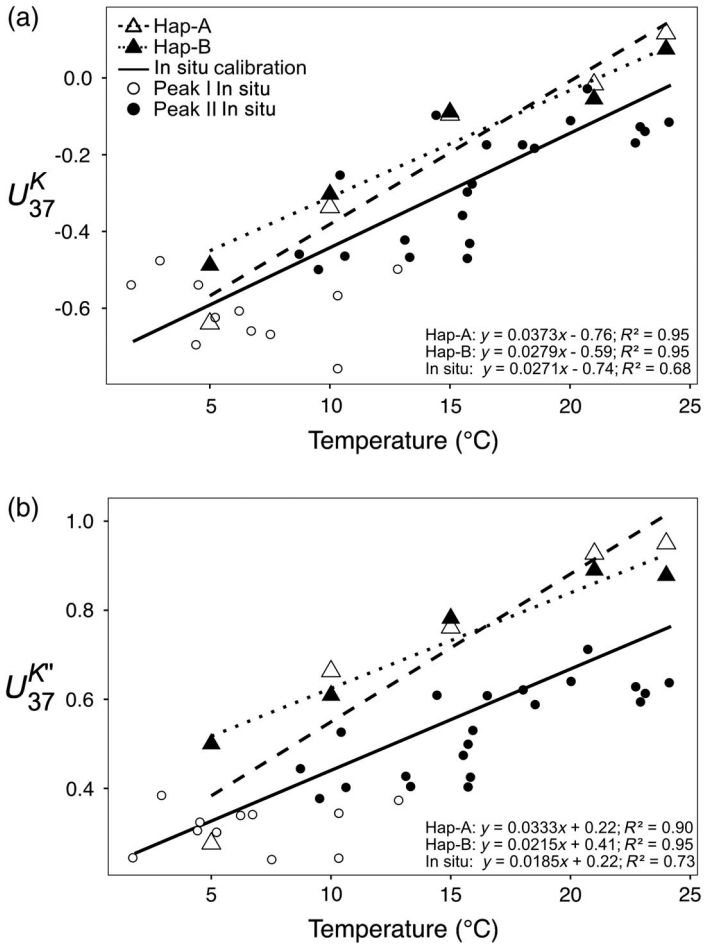

Fig. 4. U^K_{37} calibrations for the Lake George field and culture alkenones. (**a**) U^K_{37} calibrations for Lake George 2011 in situ calibration separated by Peak I and Peak II, Hap-A < 3 μm culture, and Hap-B isolate #A12,903. (**b**) As in (**a**) but with $U^{K'}_{37}$ calibration.

with which it shared 99% sequence identity (vs. 96% with Hap-A sequence #MN176134). Hap-B cells experienced a shift in morphology between the low and high temperatures, with a dominant *Ruttnera*-like (colonial) stage in the cooler temperatures and a lamellose (possessing layered sheaths) stage in the warmer temperatures (Fig. 5). The Hap-B U^K_{37} culture calibration is defined as:

$$U^K_{37} = \mathbf{0.0279\,T - 0.59} \quad (3)$$

with an R^2 value of 0.95 and a RMSE of 1.6°C. The Hap-A and Hap-B calibration curves are statistically identical and can be explained by a single curve with a composite U^K_{37} calibration as:

$$U^K_{37} = \mathbf{0.0326\,T - 0.67} \quad (4)$$

This composite culture-based calibration has an R^2 value of 0.92 and RMSE of 1.9°C. For both the Hap-A and Hap-B manipulation experiments, the fastest growth rates were observed at 15°C and alkenone per cell concentrations were highest at the coldest temperatures and lowest growth rates (Table 1).

Discussion

Haptophyte bloom successions

Lacustrine haptophyte blooms have been linked to ice-off irradiance levels following spring thaw (Toney et al. 2010; Theroux et al. 2012), similar to known triggers for annual marine blooms (Tyrrell and Merico 2004). The Lake George haptophyte bloom event began upon lake ice-off, with cool surface waters, low salinities, and low nutrient concentrations throughout the water column. Temperature and salinity gradually increased over the course of the seasonal cycle, resulting in increased water column stratification and nutrient concentration variability across the three sampling depths (Fig. 2). Across almost all sampling days, the 10 m depth water samples had higher concentrations of dissolved nitrate and phosphate, suggesting that nutrients were being sourced from the surface sediments during water column mixing or phototrophs were exhausting available nutrients in the upper photic zone.

While haptophyte viruses are known to play a key role in the termination of marine bloom events, less is known about potential haptophyte-eukaryote syntrophic or antagonistic interactions during bloom events. Lake George Hap-A abundances showed a strong positive correlation with *Chlamydomonas* species (Supporting Information Table S2), a motile, photosynthetic green alga that could be responding to the lack of stratification and limited nutrient concentrations of the late spring epilimnion. Hap-A abundances are also positively correlated with chytrid fungi (Euk_03_505, Euk_03_67), known aquatic decomposers that can operate as algal parasites (Ibelings et al. 2004). Hap-B abundances were negatively correlated with phosphate concentrations and positively correlated with a *Diacronema* (Pavlovales) haptophyte (Euk_03_140), species of which have been shown to possess a competitive advantage to other algae during low phosphate conditions (Fernández-Rodríguez et al. 2015). Future studies focused on experimental manipulations of the Lake George microbial consortium will help to better resolve these potential correlative or causative microbial interactions and to determine if Hap-A and Hap-B species exhibit competitive exclusion when cultured in tandem.

Haptophyte physiology

Previous culturing efforts revealed that an increase in irradiance levels triggered the excysting of Hap-A cells from surface sediments in sediment enrichment cultures (Toney et al. 2012). In contrast, Hap-B was grown from surface-water isolations (Toney et al. 2012; this article). A similar transition in dominant haptophyte was observed in enrichment culture experiments, with a shift from Hap-A alkenone profiles to Hap-B profiles after approximately 8 weeks (Toney et al. 2012). This ex

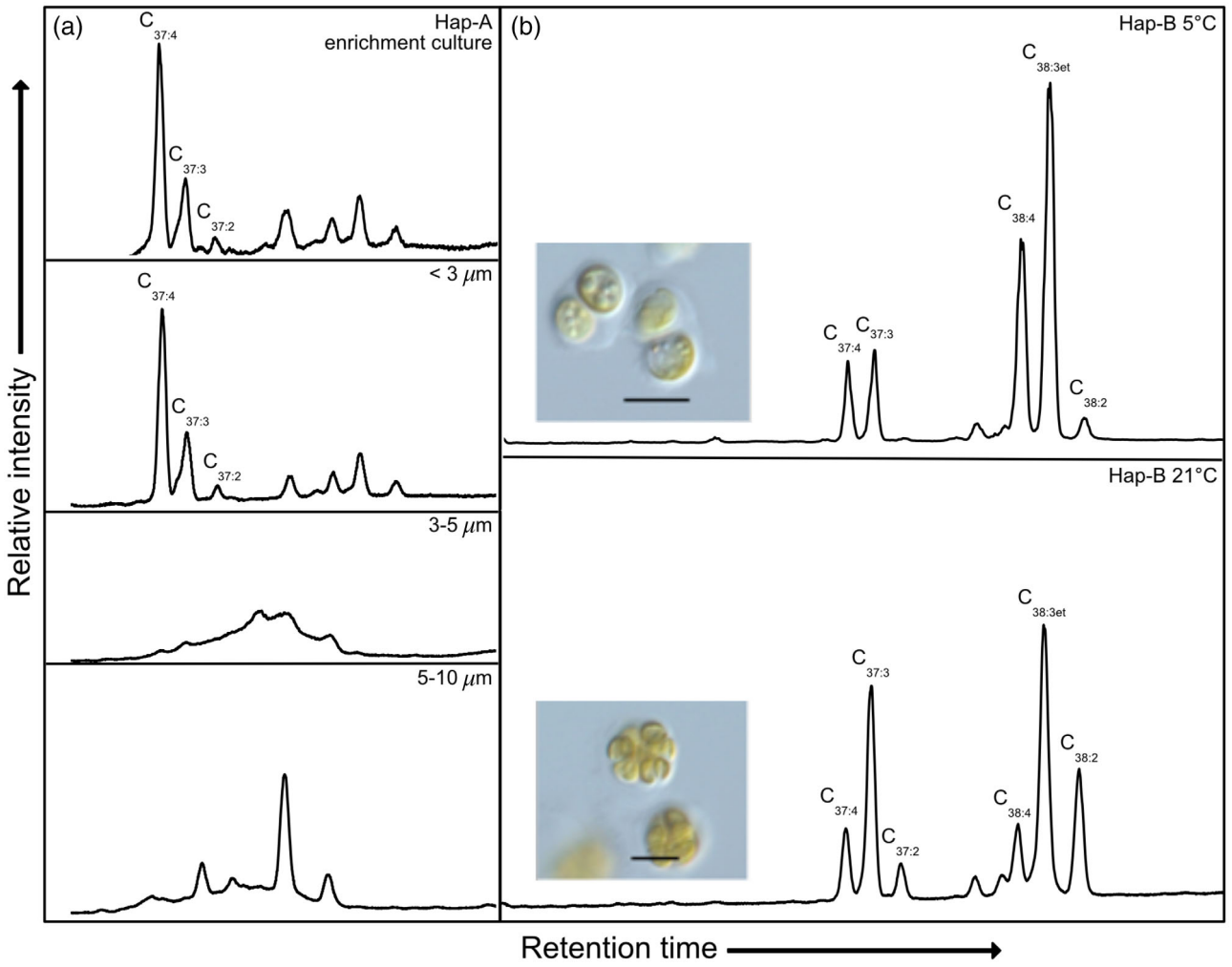

Fig. 5. Gas chromatograms of alkenone traces from Hap-A and Hap-B cultures. (**a**) Alkenone traces for Hap-A sediment enrichment culture at 5°C and size fractionation experiment indicating the source of tetraunsaturated alkenones in the < 3 μm fraction. (**b**) Hap-B strain #A12, 903 alkenones and morphology at 5°C and 21°C. Scale bar = 10 μm.

situ behavior mirrors the in situ bloom timing of the two haptophyte species: Hap-A bloomed in situ when there was an increase in light intensity following ice-off and waters were still at lower salinities and temperatures, and experiencing density-driven mixing. Hap-B cells arrived a few weeks later (Fig. 2), when temperatures were warmer and salinities were higher. In general, Hap-A read counts were negatively associated with temperature and salinity, while Hap-B read counts were positively associated with temperature, salinity, and negatively associated with nitrate and phosphate concentrations (Supporting Information Table S3).

The size fractionation experiment performed in this study revealed that Hap-A cells may be picoplanktonic for at least a portion of their life cycle (Fig. 5). Picoplankton are often found in oligotrophic waters, their high surface area to volume ratio an advantage in low nutrient conditions (Vaulot et al. 2008). However, Hap-A read counts were positively correlated with nitrate and phosphate concentrations, potentially sourced from the surface sediments during early season density-driven mixing. In contrast, Hap-B cells were negatively correlated with nutrient concentrations and appeared later in the season when nutrient concentrations were more limited. The abundance of $C_{37:4}$ alkenones observed during the Hap-A bloom and in the Hap-A cultures may suggest an ecological advantage: more unsaturated alkenones accumulate and are rapidly metabolized under nutrient-limited conditions (Epstein et al. 2001; Prahl et al. 2003; Eltgroth et al. 2005), which may explain Hap-A synthesizes these compounds and can survive extended periods of hibernation in surface sediments.

Culture-based calibrations

In agreement with previously reported *E. huxleyi*, *G. oceanica*, and *I. galbana* cultures, both Hap-A and Hap-B cultures had their lowest growth rates and highest alkenone concentrations at 5°C

Table 1. Hap-A enrichment culture and Hap-B pure culture cell counts and alkenone concentrations for the U^{K}_{37} and $U^{K'}_{37}$ calibration experiments.

	Temp. (°C)	Growth rate (div d^{-1})	Final cell count (cell mL^{-1})	Final C_{37} alkenones (ng L^{-1})	C_{37} alkenones/cell (pg)	$C_{37:4}$ (ng L^{-1})	$C_{37:3}$ (ng L^{-1})	$C_{37:2}$ (ng L^{-1})	$C_{37:4}$ (%)	U^{K}_{37}	$U^{K'}_{37}$	$U^{K''}_{37}$	K'	div d^{-1}
Hap-A	5	0.126	6.0E+04	1.0E+04	0.17	6929	2636	491	0.69	–0.64	0.16	0.28	0.09	0.13
	10	0.289	8.0E+05	2.3E+04	0.03	7876	15,465	0	0.34	–0.34	0.00	0.66	0.20	0.29
	15	0.405	5.1E+06	2.4E+04	0.00	5139	16,337	2813	0.21	–0.10	0.15	0.76	0.28	0.41
	21	0.275	6.4E+05	3.1E+04	0.05	2119	27,009	1586	0.07	–0.02	0.06	0.93	0.19	0.27
	24	0.289	8.0E+05	2.3E+04	0.03	958	18,385	3612	0.04	0.12	0.16	0.95	0.20	0.29
Hap-B	5	0.014	1.0E+04	3.3E+04	3.30	16,363	16,375	251	0.50	–0.49	0.02	0.50	0.01	0.01
	10	0.275	6.4E+05	2.4E+04	0.04	8831	13,779	1515	0.37	–0.30	0.10	0.61	0.19	0.27
	15	0.332	1.6E+06	1.8E+04	0.01	3583	12,855	1951	0.19	–0.09	0.13	0.78	0.23	0.33
	21	0.216	2.5E+05	1.8E+04	0.07	1861	15,067	884	0.10	–0.05	0.06	0.89	0.15	0.22
	24	0.229	3.1E+05	3.7E+03	0.01	367	2649	640	0.10	0.07	0.19	0.88	0.16	0.23

(Conte et al. 1998; Theroux et al. 2013). Haptophyte cultures are known to accumulate intercellular stores of alkenones during stationary growth phase and to metabolize these alkenones after being placed in the dark (Epstein et al. 2001; Eltgroth et al. 2005; Theroux et al. 2013), suggesting that alkenones serve as energy storage molecules (Epstein et al. 2001; Eltgroth et al. 2005). The accumulation of alkenones at low temperatures and low growth rates, as observed in our haptophyte cultures, is hypothesized to be the result of photosynthetic energy input exceeding the cell's capacity for growth and division (Roessler 1990). Growth rate and temperature are often conflated variables in algal batch cultures and therefore the effect on U^{K}_{37} values by increasing temperature and growth rate can be compounded (Popp et al. 1998). However, there was no consistent relationship between growth rate and U^{K}_{37} calibration across the temperature manipulation experiments in this study (Table 1).

Consistent with patterns observed in Lake George haptophyte enrichment cultures (Toney et al. 2012), the U^{K}_{37} calibrations from cultures reported in this article are offset to higher temperatures than the in situ U^{K}_{37} calibration (Fig. 4a). This offset may be the result of artificially high growth rates afforded by nutrient-rich culture conditions, which would result in more saturated, or "warmer," alkenone signatures (Popp et al. 1998). In contrast to previous culturing efforts (Toney et al. 2012), the Hap-A size-fractioned enrichment culture and the monoculture Hap-B were able to synthesize alkenones at temperatures >20°C, although both cultures exhibited a growth optimum at 15°C (Table 1). Both cultures saw a decrease in alkenone/cell concentrations with an increase in growth rate, which has implications for paleoclimate record interpretations, as discussed below.

While Hap-A produced dominant $C_{37:4}$ alkenones at 5°C, the $C_{37:3}$ alkenones were dominant at warmer temperatures. This contrasts with the alkenone signature observed in situ during the Peak I portion of the seasonal cycle, when only Hap-A reads were detected (Fig. 2). As mentioned above, the abundance of more-saturated alkenones in the isolate cultures may be a result of nutrient-replete culture conditions, which could artificially decrease the abundance of $C_{37:4}$ isomers that occur naturally during bloom conditions at similar temperatures (Fig. 4a). The Hap-A and Hap-B $U^{K'}_{37}$ calibrations, which ignore $C_{37:4}$ alkenones, did not show a relationship between alkenone unsaturation and temperature in either Hap-A or Hap-B cultures from this study, reaffirming the importance of incorporating the $C_{37:4}$ alkenone when calibrating haptophytes with naturally abundant $C_{37:4}$ (Theroux et al. 2013).

Additionally, a previously published culture-based calibration for an *R. lamellosa* isolated from Lake George resulted in a calibration (U^{K}_{37} = 0.059 T – 1.20, Zheng et al. 2016) that was distinct from the Hap-B isolate calibration from this study (Eq. 3). However, it is worth noting that the haptophyte strain isolated in this work (GenBank MN176143) and in the Zheng et al. (2016) study (KT819761) share 98% sequence similarity,

suggesting that intraspecific differences may be responsible for variability in culture-based calibrations, even when strains are maintained under similar growth conditions.

In situ calibrations

The 2011 Lake George in situ calibration (Eq. 1) yielded a calibration that was similar, although still distinct, to the Lake George 2008 in situ calibration reported previously (U^K_{37} = 0.0169 T − 0.825; Toney et al. 2012), indicating a higher y-intercept and steeper slope for the 2011 calibration reported in this study. These differences between the 2008 and 2011 Lake George in situ calibrations may reflect natural variability in cell physiology response to earlier/later ice-off, average air temperatures, and nutrient fluctuations. We recalculated the U^K_{37} for each individual sampling depth (Supporting Information Fig. S5) and found the strongest correlation between temperature and U^K_{37} at 0 and 5 m depths, suggesting most alkenones are produced in the upper portion of the photic zone. The largest scatter in the 2011 Lake George in situ U^K_{37} calibration occurred at 10°C, the temperature at which the dominant, blooming haptophyte transitioned from Hap-A to Hap-B phylotypes (Fig. 4a).

Implications for paleosalinity inferences

Previous studies have suggested the use of the $C_{37:4}$ alkenone as a paleosalinity proxy (Rosell-Melé 1998; Liu et al. 2011), with an inverse relationship between salinity and tetraunsaturated alkenone abundance. In aquatic systems like Lake George, temperature and salinity are often confounding variables, both experiencing dramatic shifts throughout a seasonal cycle. In this study, we observed a concurrent increase in temperature and salinity in the later part of summer season. The relative proportion of tetraunsaturated alkenone was inversely related to salinity (Supporting Information Fig. S5), although this relationship becomes insignificant when the influence of temperature on $C_{37:4}$ abundance is removed (Supporting Information Table S5). While salinity may have been responsible for triggering the shift from Hap-A to Hap-B populations, the relationship between $C_{37:4}$ abundance and salinity is not strong enough to warrant an independent paleosalinity proxy that is decoupled from temperature.

Implications for paleotemperature reconstructions

The majority of Lake George downcore sediments are dominated by $C_{37:4}$ alkenones (Toney et al. 2012). Based on the results of our study, the few downcore sediments with $C_{37:3}$-dominant alkenone signatures may be the result of environmental conditions favoring Hap-B productivity, such as warmer water temperatures or higher salinities. During the 2011 Lake George haptophyte bloom, the Peak II, Hap-B-dominated surface waters experienced higher concentrations of C_{37} alkenones than those observed during the Hap-A-dominant Peak I (Fig. 2). This result is surprising, given a sediment record that is dominated by $C_{37:4}$ alkenones. There are few scenarios that could result in a $C_{37:4}$ dominant sediment record: (1) Hap-A cells were more productive in previous bloom seasons, resulting in greater $C_{37:4}$ deposition in the sediment record, or (2) Hap-B cells were subject to greater grazing pressure and their alkenone signatures were not preserved in the sediment record. It is unlikely that the $C_{37:4}$-dominant sediment record is the result of alkenone production by Hap-A cells while still in the surface sediments, as this mode of production would result in a steady, cold-water alkenone signature, in addition to the fact that surface sediments are out of the photic zone and the haptophyte cells would be forced to metabolize, as opposed to synthesize, their alkenones. Regarding the possibility of below-ice alkenone production, previous studies in Lake George (Toney et al. 2010) and Lake BrayaSø, Greenland (D'Andrea et al. 2011) did not detect alkenone production in the water column or export to the surface sediments while the lakes were ice-covered, supporting the conclusion that alkenone production occurs primarily during the ice-free bloom season. There is also the possibility that Hap-A cells in the sediments are able to photosynthesize in shallow regions of the lake, with these alkenones being laterally transported via resuspension and transport (as in Eadie et al. 2008). The production of alkenones in shallow waters with on-average warmer temperatures is another potential scenario that should be considered when establishing the provenance of alkenones deposited in lake surface sediments.

This study is the first to demonstrate a shared U^K_{37} between genetically distinct haptophytes in a single lake and offers an optimistic outlook for lake paleotemperature reconstruction in the presence of multiple alkenone-producing haptophytes. As observed in this study, both haptophyte cultures demonstrated a decreasing alkenone/cell concentration with increasing growth rates, indicating that alkenone concentrations in sediment records are not necessarily indicative of haptophyte growth rates. Bloom timing, alkenone/cell concentrations, and alkenone export to the surface sediments are all key variables in dictating the eventual composition of the alkenone sediment record.

Conclusions

This study provides new insights into lacustrine haptophyte physiology, ecology, and bloom conditions. As evidenced by a shift in both alkenone and DNA signatures in the water column, the Lake George seasonal cycle consisted of two subsequent haptophyte blooms by two separate haptophyte species. Haptophyte species Hap-A was the dominant haptophyte during the spring Peak I bloom event, when water alkenone signatures were dominated by $C_{37:4}$ alkenones. The summer bloom event was characterized by the presence of the Hap-B species and water alkenone signatures dominated by $C_{37:3}$ alkenones. While the exact environmental triggers for the bloom events remain unclear, the spring thaw may induce the

excysting of Hap-A, while temperature, salinity, and stratification shifts may support the transition to Hap-B dominance in the surface waters. Culture-based U^K_{37} calibrations for the two haptophyte species in Lake George were statistically identical and biased to higher U^K_{37} values, potentially the result of artificially nutrient-rich conditions in culture. Alkenone-based temperature reconstruction from lake records must therefore consider the multifactor influence of haptophyte bloom timing, succession, strength, and preservation when interpreting these valuable paleoclimate archives. Future studies into the environmental and biological triggers of lake-dwelling haptophyte blooms will help to better refine our understanding of the seasonality of alkenone production and its influence on the paleotemperature record.

References

Amaral-Zettler, L. A., E. A. McCliment, H. W. Ducklow, and S. M. Huse. 2009. A method for studying protistan diversity using massively parallel sequencing of V9 hypervariable regions of small-subunit ribosomal RNA genes. PLoS One **4**: e6372. doi:10.1371/journal.pone.0006372

Araie, H., and others. 2018. Novel alkenone-producing strains of genus *Isochrysis* (Haptophyta) isolated from Canadian saline lakes show temperature sensitivity of alkenones and alkenoates. Org. Geochem. **121**: 89–103. doi:10.1016/j.orggeochem.2018.04.008

Bendif, E. M., I. Probert, D. C. Schroeder, and C. de Vargas. 2013. On the description of *Tisochrysis lutea* gen. nov. sp. nov. and *Isochrysis nuda* sp. nov. in the *Isochrysidales*, and the transfer of *Dicrateria* to the Prymnesiales (Haptophyta). J. Appl. Phycol. **25**: 1763–1776. doi:10.1007/s10811-013-0037-0

Brassell, S. C., G. Eglinton, I. T. Marlowe, U. Pflaumann, and M. Sarnthein. 1986. Molecular stratigraphy: A new tool for climatic assessment. Nature **320**: 129–133. doi:10.1038/320129a0

Conte, M. H., A. Thompson, D. Lesley, and R. P. Harris. 1998. Genetic and physiological influences on the alkenone/alkenoate vs. growth temperature relationship in *Emiliania huxleyi* and *Gephyrocapsa oceanica*. Geochim. Cosmochim. Acta **62**: 51–68. doi:10.1016/S0016-7037(97)00327-X

Conte, M. H., M. A. Sicre, C. Rühlemann, J. C. Weber, S. Schulte, D. Schulz-Bull, and T. Blanz. 2006. Global temperature calibration of the alkenone unsaturation index ($U^{K'}_{37}$) in surface waters and comparison with surface sediments. Geochem. Geophys. Geosyst. **7**: Q02005. doi:10.1029/2005GC001054

Coolen, M. J. L., G. Muyzer, W. I. C. Rijpstra, S. Schouten, J. K. Volkman, and J. S. Sinninghe Damsté. 2004. Combined DNA and lipid analyses of sediments reveal changes in Holocene haptophyte and diatom populations in an Antarctic lake. Earth Planet. Sci. Lett. **223**: 225–239. doi:10.1016/j.epsl.2004.04.014

Coolen, M. J. L., J. P. Saenz, L. Giosan, N. Y. Trowbridge, P. Dimitrov, D. Dimitrov, and T. I. Eglinton. 2009. DNA and lipid molecular stratigraphic records of haptophyte succession in the Black Sea during the Holocene. Earth Planet. Sci. Lett. **284**: 610–621. doi:10.1016/j.epsl.2009.05.029

D'Andrea, W. J., M. Lage, J. B. H. Martiny, A. D. Laatsch, L. A. Amaral-Zettler, M. L. Sogin, and Y. Huang. 2006. Alkenone producers inferred from well-preserved 18S rDNA in Greenland lake sediments. J. Geophys. Res. Biogeosci. **111**: G03013. doi:10.1029/2005JG000121

D'Andrea, W. J., Y. Huang, S. C. Fritz, and N. J. Anderson. 2011. Abrupt Holocene climate change as an important factor for human migration in West Greenland. Proc. Natl. Acad. Sci. USA **108**: 9765–9769. doi:10.1073/pnas.1101708108

Dillon, J. T., W. M. Longo, Y. Zhang, R. Torozo, and Y. Huang. 2016. Identification of double-bond positions in isomeric alkenones from a lacustrine haptophyte. Rapid Commun. Mass Spectrom. **30**: 112–118. doi:10.1002/rcm.7414

Eadie, B., J. Robbins, J. V. Klump, D. Schwab, and D. Edgington. 2008. Winter–spring storms and their influence on sediment resuspension, transport, and accumulation patterns in southern Lake Michigan. Oceanography **21**: 118–135. doi:10.5670/oceanog.2008.09

Eisenlohr, W., and C. Sloan. 1968. Generalized hydrology of prairie potholes on the Coteau du Missouri, North Dakota, p. 12. Geol. Surv. Circ. 558. doi:10.3133/cir558

Eltgroth, M. L., R. L. Watwood, and G. V. Wolfe. 2005. Production and cellular localization of neutral long-chain lipids in the haptophyte algae *Isochrysis galbana* and *Emiliania huxleyi*. J. Phycol. **41**: 1000–1009. doi:10.1111/j.1529-8817.2005.00128.x

Epstein, B. L., S. D'Hondt, and P. E. Hargraves. 2001. The possible metabolic role of C_{37} alkenones in *Emiliania huxleyi*. Org. Geochem. **32**: 867–875. doi:10.1016/S0146-6380(01)00026-2

Fernández-Rodríguez, M. J., C. Hidalgo-Lara, A. Jiménez-Rodríguez, and L. Serrano. 2015. Bloom-forming microalgae in high-species phytoplankton assemblages under light-fluctuating and low phosphate conditions. Estuaries Coast. **38**: 1642–1655. doi:10.1007/s12237-014-9891-5

Fritz, S. 2011. Lake George and its geological history during the last ~10,000 years, p. 1–3. CGREC annual report. North Dakota State University.

Guillard, R. R. L. 1975. Culture of phytoplankton for feeding marine invertebrates, p. 29–60. *In* W. L. Smith and M. H. Chanley [eds.], Culture of marine invertebrate animals: Proceedings—1st Conference on Culture of Marine Invertebrate Animals Greenport. Springer, Boston, MA. doi:10.1007/978-1-4615-8714-9_3

Huse, S. M., J. A. Huber, H. G. Morrison, M. L. Sogin, and D. Mark Welch. 2007. Accuracy and quality of massively parallel DNA pyrosequencing. Genome Biol. **8**: R143. doi:10.1186/gb-2007-8-7-r143

Huse, S. M., L. Dethlefsen, J. A. Huber, D. Mark Welch, D. A. Relman, and M. L. Sogin. 2008. Exploring microbial

diversity and taxonomy using SSU rRNA hypervariable tag sequencing. PLoS Genet. **4**: e1000255. doi:10.1371/journal.pgen.1000255

Huse, S. M., D. M. Welch, H. G. Morrison, and M. L. Sogin. 2010. Ironing out the wrinkles in the rare biosphere through improved OTU clustering. Environ. Microbiol. **12**: 1889–1898. doi:10.1111/j.1462-2920.2010.02193.x

Ibelings, B. W., A. De Bruin, M. Kagami, M. Rijkeboer, M. Brehm, and E. V. Donk. 2004. Host parasite interactions between freshwater phytoplankton and chytrid fungi (Chytridiomycota). J. Phycol. **40**: 437–453. doi:10.1111/j.1529-8817.2004.03117.x

Liu, W., Z. Liu, H. Wang, Y. He, Z. Wang, and L. Xu. 2011. Salinity control on long-chain alkenone distributions in lake surface waters and sediments of the northern Qinghai-Tibetan Plateau, China. Geochim. Cosmochim. Acta **75**: 1693–1703. doi:10.1016/j.gca.2010.10.029

Longo, W. M., J. T. Dillon, R. Tarozo, J. M. Salacup, and Y. Huang. 2013. Unprecedented separation of long chain alkenones from gas chromatography with a poly(trifluoropropylmethylsiloxane) stationary phase. Org. Geochem. **65**: 94–102. doi:10.1016/j.orggeochem.2013.10.011

Longo, W. M., S. Theroux, A. E. Giblin, Y. Zheng, J. T. Dillon, and Y. Huang. 2016. Temperature calibration and phylogenetically distinct distributions for freshwater alkenones: Evidence from northern Alaskan lakes. Geochim. Cosmochim. Acta **180**: 177–196. doi:10.1016/j.gca.2016.02.019

Marlowe, I. T., J. C. Green, A. C. Neal, S. C. Brassell, G. Eglinton, and P. A. Course. 1984. Long chain (n-C37–C39) alkenones in the Prymnesiophyceae. Distribution of alkenones and other lipids and their taxonomic significance. British Phycological Journal **19**: 203–216. doi:10.1080/00071618400650221

Müller, P. J., G. Kirst, G. Ruhland, I. Von Storch, and A. Rosell-Melé. 1998. Calibration of the alkenone paleotemperature index $U^{K'}_{37}$ based on core-tops from the eastern South Atlantic and the global ocean (60°N-60°S). Geochim. Cosmochim. Acta **62**: 1757–1772. doi:10.1016/S0016-7037(98)00097-0

Nakamura, H., K. Sawada, H. Araie, T. Shiratori, K. Ishida, I. Suzuki, and Y. Shiraiwa. 2016. Composition of long chain alkenones and alkenoates as a function of growth temperature in marine haptophyte *Tisochrysis lutea*. Org. Geochem. **99**: 78–89. doi:10.1016/j.orggeochem.2016.06.006

Popp, B. N., F. Kenig, S. G. Wakeham, E. A. Laws, and R. R. Bidigare. 1998. Does growth rate affect ketone unsaturation and intracellular carbon isotopic variability in *Emiliania huxleyi*? Paleoceanography **13**: 35–41. doi:10.1029/97PA02594

Prahl, F. G., and S. G. Wakeham. 1987. Calibration of unsaturation patterns in long-chain ketone compositions for palaeotemperature assessment. Nature **330**: 367–369. doi:10.1038/330367a0

Prahl, F. G., L. A. Muehlhausen, and D. L. Zahnle. 1988. Further evaluation of long-chain alkenones as indicators of paleoceanographic conditions. Geochim. Cosmochim. Acta **52**: 2303–2310. doi:10.1016/0016-7037(88)90132-9

Prahl, F. G., M. A. Sparrow, and G. V. Wolfe. 2003. Physiological impacts on alkenone paleothermometry. Paleoceanography **18**: 1025. doi:10.1029/2002PA000803

R Core Team. 2013. R: A language and environment for statistical computing. Foundation for Statistical Computing, Vienna, Austria. (accessed 2019 February 19). Available from http://www.R-project.org/

Roessler, P. G. 1990. Environmental control of glycerolipid metabolism in microalgae: Commercial implications and future research directions. J. Phycol. **26**: 393–399. doi:10.1111/j.0022-3646.1990.00393.x

Rosell-Melé, A. 1998. Interhemispheric appraisal of the value of alkenone indices as temperature and salinity proxies in high-latitude locations. Paleoceanography **13**: 694–703. doi:10.1029/98PA02355

Simon, M., P. Lopez-Garcia, D. Moreira, and L. Jardillier. 2013. New haptophyte lineages and multiple independent colonizations of freshwater ecosystems. Environ. Microbiol. Rep. **5**: 322–332. doi:10.1111/1758-2229.12023

Sun, Q., G. Chu, G. Liu, S. Li, and X. Wang. 2007. Calibration of alkenone unsaturation index with growth temperature for a lacustrine species, *Chrysotila lamellosa* (Haptophyceae). Org. Geochem. **38**: 1226–1234. doi:10.1016/j.orggeochem.2007.04.007

Theroux, S., W. J. D'Andrea, J. Toney, L. Amaral-Zettler, and Y. Huang. 2010. Phylogenetic diversity and evolutionary relatedness of alkenone-producing haptophyte algae in lakes: Implications for continental paleotemperature reconstructions. Earth Planet. Sci. Lett. **300**: 311–320. doi:10.1016/j.epsl.2010.10.009

Theroux, S., Y. Huang, and L. Amaral-Zettler. 2012. Comparative molecular microbial ecology of the spring haptophyte bloom in a Greenland Arctic oligosaline lake. Front. Microbiol. **3**: 415. doi:10.3389/fmicb.2012.00415

Theroux, S., J. Toney, L. Amaral-Zettler, and Y. Huang. 2013. Production and temperature sensitivity of long chain alkenones in the cultured haptophyte *Pseudoisochrysis paradoxa*. Org. Geochem. **62**: 68–73. doi:10.1016/j.orggeochem.2013.07.006

Toney, J. L., Y. Huang, S. C. Fritz, P. A. Baker, E. Grimm, and P. Nyren. 2010. Climatic and environmental controls on the occurrence and distributions of long chain alkenones in lakes of the interior United States. Geochim. Cosmochim. Acta **74**: 1563–1578. doi:10.1016/j.gca.2009.11.021

Toney, J. L., S. Theroux, R. A. Andersen, A. Coleman, L. Amaral-Zettler, and Y. Huang. 2012. Culturing of the first 37:4 predominant lacustrine haptophyte: Geochemical,

biochemical, and genetic implications. Geochim. Cosmochim. Acta **78**: 51–64. doi:10.1016/j.gca.2011.11.024

Tyrrell, T., and A. Merico. 2004. *Emiliania huxleyi*: Bloom observations and the conditions that induce them, p. 75–97. *In* H. R. Thierstein and J. R. Young [eds.], Coccolithophores: From molecular processes to global impact. Springer. doi:10.1007/978-3-662-06278-4_4

Vaulot, D., W. Eikrem, M. Viprey, and H. Moreau. 2008. The diversity of small eukaryotic phytoplankton (< or = 3 microm) in marine ecosystems. FEMS Microbiol. Rev. **32**: 795–820. doi:10.1111/j.1574-6976.2008.00121.x

Versteegh, G. J. M., R. Riegman, J. W. de Leeuw, and J. H. F. F. Jansen. 2001. $U^{K'}_{37}$ values for *Isochrysis galbana* as a function of culture temperature, light intensity and nutrient concentrations. Org. Geochem. **32**: 785–794. doi:10.1016/S0146-6380(01)00041-9

Volkman, J. K., G. Eglinton, E. D. S. Corner, and T. E. V. Forsberg. 1980. Long-chain alkenes and alkenones in the marine coccolithophorid *Emiliania huxleyi*. Phytochemistry **19**: 2619–2622. doi:10.1016/S0031-9422(00)83930-8

Volkman, J. K., S. M. Barrett, S. I. Blackburn, and E. L. Sikes. 1995. Alkenones in *Gephyrocapsa oceanica* - implications for studies of paleoclimate. Geochim. Cosmochim. Acta **59**: 513–520. doi:10.1016/0016-7037(95)00325-T

Whitehead, R. L. 1996. Ground water atlas of the United States: Segment 8, Montana, North Dakota, South Dakota, Wyoming (USGS numbered series No. 730– I). Hydrologic atlas. U.S. Geological Survey. doi:10.3133/ha730I

Yilmaz, P., and others. 2011. Minimum information about a marker gene sequence (MIMARKS) and minimum information about any (x) sequence (MIxS) specifications. Nat. Biotechnol. **29**: 415–420. doi:10.1038/nbt.1823

Zheng, Y., Y. Huang, R. A. Andersen, and L. A. Amaral-Zettler. 2016. Excluding the di-unsaturated alkenone in the U^{K}_{37} index strengthens temperature correlation for the common lacustrine and brackish-water haptophytes. Geochim. Cosmochim. Acta **175**: 36–46. doi:10.1016/j.gca.2015.11.024

Acknowledgments

We thank Mara Freilich for support with in situ calibration experiments, Jingwei Ni from Life Technologies for Ion Torrent bioinformatics support, and Jason Affourtit from Life Technologies for coordinating this assistance. Sharon Grimm, Hilary Morrison, and Beth Slikas provided technical advice and assistance with sequencing and data processing. This work was supported by a National Science Foundation award to Y. Huang (EAR-1122749) and L. Amaral-Zettler (EAR-1124192), a Brown University SEED fund to Y. Huang and L. Amaral-Zettler, and an American Association of University Women dissertation fellowship to S. Theroux.

Conflict of Interest

None declared.

Submitted 25 March 2019
Revised 18 July 2019
Accepted 01 August 2019

Associate editor: Heidi Sosik